LA-UR-95- 100

Title: Bubble Fusion: Preliminary Estimates

Author(s): R. A. Krakowski

Submitted to: General Distribution

DISCLAIMER

This report was prepared as an account of work sponsored by an agency of the United States Government. Neither the United States Government nor any agency thereof, nor any of their employees, makes any warranty, express or implied, or assumes any legal liability or responsibility for the accuracy, completeness, or usefulness of any information, apparatus, product, or process disclosed, or represents that its use would not infringe privately owned rights. Reference herein to any specific commercial product, process, or service by trade name, trademark, manufacturer, or otherwise does not necessarily constitute or imply its endorsement, recommendation, or favoring by the United States Government or any agency thereof. The views and opinions of authors expressed herein do not necessarily state or reflect those of the United States Government or any agency thereof.

MASTER

Los Alamos
NATIONAL LABORATORY

Los Alamos National Laboratory, an affirmative action/equal opportunity employer, is operated by the University of California for the U.S. Department of Energy under contract W-7405-ENG-36. By acceptance of this article, the publisher recognizes that the U.S. Government retains a nonexclusive, royalty-free license to publish or reproduce the published form of this contribution, or to allow others to do so, for U.S. Government purposes. The Los Alamos National Laboratory requests that the publisher identify this article as work performed under the auspices of the U.S. Department of Energy.

DISTRIBUTION OF THIS DOCUMENT IS UNLIMITED

Form No. 836 R5
ST 2629 10/91

DISCLAIMER

Portions of this document may be illegible in electronic image products. Images are produced from the best available original document.

BUBBLE FUSION: PRELIMINARY ESTIMATES

by

R. A. Krakowski
January 4, 1995

ABSTRACT

The collapse of a gas-filled bubble in disequilibrium (*i.e.,* internal pressure << external pressure) can occur with a significant focusing of energy onto the entrapped gas in the form of pressure-volume work and/or acoustical shocks; the resulting heating can be sufficient to cause ionization and the emission of atomic radiations. The suggestion that extreme conditions necessary for thermonuclear fusion to occur may be possible has been examined parametrically in terms of the ratio of initial bubble pressure relative to that required for equilibrium. In this sense, the disequilibrium bubble is viewed as a three-dimensional "sling shot" that is "loaded" to an extent allowed by the maximum level of disequilibrium that can stably be achieved. Values of this disequilibrium ratio in the range 10^{-5}–10^{-6} are predicted by an idealized bubble-dynamics model as necessary to achieve conditions where nuclear fusion of deuterium-tritium might be observed. Harmonic and aharmonic pressurizations/decompressions are examined as means to achieve the required levels of disequilibrium required to create fusion conditions. A number of phenomena not included in the analysis reported herein could enhance or reduce the small levels of nuclear fusions predicted.

I. INTRODUCTION

Liquids exposed to intense ultrasonic waves can generate small cavities or bubbles that upon expansion and subsequent implosion create strong local heating. Studies of acousto-chemical or sonochemical reactions induced by this strong local heating have been recently reported[1-2] and thoroughly reviewed.[4-10] Although temperatures of 10,000s K have been reported, extension of these sonochemical conditions to those required to induce thermonuclear fusion have also been suggested.[1,7,11] To examine the latter possibility, the standard (simplified) bubble-dynamics equation[4,8,12,13] has been solved parametrically in the context of DT fusion, and projections are reported herein. This parametric analysis is based on modeling the dynamics of a cavity filled with a (nearly) ideal gas (g) and vapor (v); the gas-filled cavity is subject to a constant hydrostatic (h) pressure and an oscillatory externally applied pressure (a). While a van der Waals equation of state is used and free-electron (Bremsstrahlung) radiation losses are included, the generally optimistic assumptions of no gradient-driven transport, no gas/plasma interactions with the cavity wall, and completely stable spherical implosions are invoked.

While the impact of gas-phase shock waves launched from the inward-moving spherical piston are not included in this analysis, the creation and interactions of these cavity-wall

launched and reflected shocks has been suggested[14-16] as one explanation for the timing and location of sonoluminescence observed under some conditions. Other explanations for the radiation observed to accompany bubble collapse include collision-induced emission from dipoles[17] and Casimir energy[18] released when a dielectric hole (*i.e.*, the cavity) is filled.[19] The latter two explanations would preclude conditions where nuclear fusion of light elements might occur, whereas the modeling multiply interacting, reactive shocks is an area for future work; the present "scoping" calculations, therefore, are based on modeling uniform, nearly adiabatic compressional heating of a hard-sphere gas in a collapsing cavity using a formalism that differs little from that reported by Lord Rayleigh nearly eighty years ago[20].

The collapse of a gas-filled bubble with an internal gas pressure $P_{go} << P_h$ was simply and accurately modeled in 1917 by Lord Rayleigh[20], who suggested that the potential energy $\sim(4/3)\,R_o^3\,(P_h - P_{go})$ created by the formation of a non-equilibrium cavity of radius R_o in a hydrostatically pressurized liquid at a pressure P_h could be converted to kinetic energy of all the surrounding liquid and focused onto the gas trapped in the cavity of ever-diminishing radius R(t). This "disequilibrium" bubble (*e.g.*, $f_{eq} = P_{go}/P_{go}^{EQ} << 1$, where P_{go}^{EQ} is the gas pressure needed to achieve force balance with the environment) can be viewed as a three-dimensional "sling shot", cocked and ready to convert the elastically stored potential energy in the liquid and to perform pressure-volume work on the contained gas.

The first part of the analysis reported herein parametrically describes in a fusion context (*e.g.*, fusion neutron yield, density-time-temperature product) the effect of varying the loading of this three-dimensional "sling shot" *vis á vis* the disequilibrium parameter f_{eq}. The feasibility of achieving the required level of disequilibrium starting with an equilibrium bubble (*e.g.*, $f_{eq} = 1$) is then investigated by solving the bubble-dynamics equation under conditions of both harmonic and aharmonic/resonant pressure loading of the liquid surrounding the (initially) equilibrium bubble. The main goal of this study is to understand better conditions where deuterium-tritium fusions might be observed; not even a hint of a prognoses for practical application is intended at this point.

II. MODEL

A gas-filled bubble in pressure equilibrium between forces associated with a uniform hydrostatic pressure, P_h, vapor pressure in the cavity associated with the surrounding liquid, P_v, the surface-tension or Laplace pressure, $P_\sigma = 2\sigma/R$, and the internal (insoluable) gas pressure, P_g, is describe for a bubble of radius R relative to some reference radius R_o as follows:

$$P_h = (P_{ho} + P_{\sigma o} - P_v)z^\gamma + P_v - P_{\sigma o}\,z \ , \qquad (1)$$

where $z = (R_o/R)^3$ is the compression ratio, and the subscript "o" refers to a reference (initial) equilibrium conditions (*e.g.*, $P_{go}^{EQ} = P_{ho} + P_{\sigma o} - P_v$), the cavity wall is assumed to be isothermal (*e.g.*, the vapor pressure, P_v, is assumed to be constant), and an ideal gas

with polytropic exponent γ are assumed. The parameter $f_{eq} = P_{go}/P_{go}^{EQ}$ is introduced as a measure of initial force or pressure "disequilibrium" within the gas bubble. While the path to this "disequilibrium" is left unspecified in the first part of the parametric analysis, the (starting) pressure $P_{go} = f_{eq} P_{go}^{EQ}$ does not satisfy the equilibrium described by Eqn. (1), and for $f_{eq} < 1$ the bubble will collapse under the force of this disequilibrium.[20] The potential energy associated with this disequilibrium bubble of (initial) radius R_o emersed in a liquid under hydrostatic pressure P_h is given by

$$(PE)_i = (4/3)\pi[R_o^3 - (R_o^{EQ})^3]P_h \quad . \tag{2}$$

As this $f_{eq} < 1$ disequilibrium bubble collapses, the potential energy relative to $(PE)_i$ is described by

$$PE = (4/3)\pi(R_o^3 - R^3)P_h \quad , \tag{3}$$

and the kinetic energy of the inward-moving liquid surrounding the collapsing bubble is summed up over all radii $r > R(t)$ as follows:

$$KE = \int_R^\infty \frac{1}{2}(4\pi r^2 \rho_\ell \, dr)(dr/dt)^2 \quad , \tag{4}$$

where the radial coordinate r is associated with the liquid. Including the work expended in adiabatically compressing the gas entrapped within the bubble [for an ideal gas, $P_g/z^\gamma =$ constant, work $= P_{go}V_o\{z^{\gamma-1} - 1\}/(\gamma - 1)$ for $\gamma > 1$ or $P_{go}V_o \, \ell n \, z$ for $\gamma = 1$], along with the assumption of incompressibility of the host liquid [*e.g.*, $4\pi r^2 (dr/dt) = 4\pi R^2 (dR/dt)$], the following bubble kinetics equation results from the balance of KE, PE, and pressure-volume work[13,20]:

$$\frac{3}{2}\left[\frac{dR/dr}{\omega_R \; R-o}\right]^2 = z - 1 - \frac{3}{2}\frac{P_{\sigma o}}{P_h}[z - z^{1/3}] - \frac{P_{go}}{P_h} g(z) \quad , \tag{5}$$

where

$$g(z) = \begin{cases} z \; \ell n(z) & (\gamma = 1) \\ \dfrac{z^{\gamma-1} - 1}{\gamma - 1} & (\gamma > 1) \end{cases} \quad , \tag{6}$$

and $\omega_r = \sqrt{(P_h/\rho_\ell)}/R_o$ is the natural (resonant) frequency of the initial (disequilibrium) bubble. For the case where $P_{\sigma o} = P_{go} = 0$, the time for the disequilibrium collapse, $\tau^* = \int_{R_o}^{R} dr/(dR/dt)$, is given by[20]

$$\omega_R \tau^* = \sqrt{\frac{3}{2}} \int_1^{z_{max} \simeq \infty} \frac{dz}{3\, z^{1/6} \sqrt{1 - z}}$$

$$= \frac{1}{\sqrt{6}} \frac{\Gamma(5/6)\ \Gamma(1/2)}{\Gamma(4/3)} = 0.9146 \ , \tag{7}$$

where $\Gamma(y) = \int_0^\infty e^{-x}\ x^{y-1}\, dx$ is the Gamma Function. Lastly, the "impulse parameter", $\int P_g dt$, is expressed below in "fusion units," $n(1/m^3)$, $\tau(s)$, and $T_{keV}(keV)$:

$$< n \tau T_{keV} > (s\ \ keV/m^3) = \frac{N_A\ k_B}{R_G} \frac{P_{go}}{\omega_r} \int_1^{z_{max}} \frac{z^{\gamma - 4/3}\, dz}{(dR/dt)/(\omega_r R_o)} \ . \tag{8}$$

When a time-varying pressure, $P_a(t)$, is added to the hydrostatic pressure, P_h, far from the bubble and included in the balance between kinetic energy, potential energy, and work, along with the addition of a viscous pressure term[13] $[-4 \eta R^2 (dR/dt)/r]$ to P_h, and using the relative pressure balance described by Eqn. (1), the following (Rayleigh-Plesset) bubble-dynamics equation results:

$$\rho_l \left[R \frac{dv}{dt} + \frac{3}{2} v^2 \right] = (P_h + P_{\sigma o} - P_v) z^\gamma + P_v z^{1/3}$$

$$- \frac{4\ \eta\ v\ z^{1/3}}{R_o} - P_h - P_a(t) \ , \tag{9}$$

where $v = dR/dt$. The Rayleigh-Plesset (Noltingk-Neppiras-Poritsky)[13] equation describes a highly idealized bubble and is subject to a number of important limitation, some of which are listed below[4,10,13]:

- single bubble in an infinite medium
- spherical bubble, no distortions or breakup
- spatially uniformity within and outside the bubble
- absence of body forces
- acoustic wavelengths (associated with P_a) much greater than R
- no viscous effects within the bulk liquid [the term in Eqn. (9) is associated only with fluid motion near the bubble surface]
- incompressible liquid phase
- constant gas inventory within the bubble
- constant liquid vapor pressure (isothermal cavity wall)
- no molecular diffusion into or out of the bubble
- no acoustic streaming and impact of resulting shear stresses on bubble shape

- ideal-gas, adiabatic behavior within the bubble with a constant polytropic coefficient.
- no radiation loss from the gas/plasma within the bubble
- no gas-phase shock formation (c >> dR/dt).

With these limitations in mind, Eqn. (9) is solved for both a sinusoidal ($P_a = P_A \sin \omega t$) and an aharmonic/resonant pressure function, [$P_a(t) = P_A\, 2^{N-1}$ for the N^{th} compression in a series of compression-expansion cycles], starting with an equilibrium bubble ($x_o = R_o/R_o^{EQ} = 1$, $f_{eq} = 1$). In the case of driven systems, an initial radius, R_o^{EQ}, is chosen to give a natural resonant frequency, ω_r, equal to the driver frequency, $2\pi f$; otherwise, a significant part of the numerical computation is devoted to resolving uninteresting transient oscillations[23]. In addition to determining R(t) and T(t), the resulting gas pressure, $P_g(t)$ is assumed to be generated in a deuterium- tritium (DT) gas mixture, an impulse parameter $<n \tau T_{keV}>$ is computed for each compression the arises, and the DT fusion yield

$$YLD = \int_o^t \frac{1}{4}\, n^2 <\sigma v>\, dt\, (4/3)\, \pi\, R^3\, dt\ , \qquad (10)$$

for each compression registered, where $n = \rho_g N_A$ and $<\sigma v>$ is the DT fusion reactivity. These integral quantities, along with the peak radial compression, $x_{min} = R_{min}/R_o$, and the maximum temperature, $T(x_{min})$, are correlated with the disequilibrium parameter, $f_{eq} = P_{go}/P_{go}^{EQ}$, evaluated at the beginning of each major compression.

Both DT depletion through burnup and fusion-product heating are monitored, but this information is not incorporated into the time-dependent model; for most of the conditions examined, these fusion-related effects on the bubble dynamics and response are not important.

Although most of the approximations listed above are retained in the present analysis, the following van der Waals equation of state replaces the ideal-gas assumption:

$$P(v - v_H) = R_G \qquad (11)$$

$$w = c_v T = (v - v_H)\, P/(\gamma - 1) \qquad (12)$$

$$P(v - v_H) = S/c_v\ , \qquad (13)$$

where $v = 1/\rho_g$ is the specific volume of the gas and $v_H = 0.05\ m^3/kmole$ is the "hard-sphere" volume of the hydrogen atom. In this case the ideal-gas adiabatic is subject to the following correction:

$$\frac{P}{P_o}\, x^{3\gamma} = \frac{1}{f_{VDW}} \qquad (14)$$

$$f_{VDW} = \left[\frac{1 - v_H^*/x^3}{1 - v_H^*}\right]^{\gamma} , \tag{15}$$

where $v_H^* = \rho_{go} v_H$ and $\rho_{go} = P_{go}/(R_G T_o)$ is the initial pressure gas pressure in the bubble.

A second correction to the ideal-gas adiabatic is applied to adjust (approximately) for "sliding adiabaticity" associated with energy shed from the compressing bubble from free-electron (Bremsstrahlung) radiation. In this case, the right-hand side of Eqn. (14) is multiplied by the factor $e^{-I(t)}$, where the integral I(t) is given by

$$I(t) = \int_o^t \frac{p_{RAD}}{w}\, dt , \tag{16}$$

and

$$p_{RAD}(W/m^3) = C_{BR}\,(Z\ f_{ion}\ n)^2\, T_{keV}^{1/2} \tag{17}$$

$$w(J/m^3) = \frac{3}{2}(1 + f_{ion}) k_B\, T\, n . \tag{18}$$

The radiation power density and the total energy density in the bubble are p_{RAD} and w, respectively. The degree of ionization, f_{ion}, is assumed to be given by the Saha equilibrium relationship[21,22]

$$f_{ion} = \frac{1}{1 + \sqrt{(1 + 4/K)}} \tag{19}$$

$$K = \frac{2Q_1}{Q_0}\left[\frac{2\ \pi\ m_e\ e}{h^2}\right]^{3/2}\left[\frac{T_{eV}}{n}\right]^{3/2} e^{-E_i/T_{eV}} . \tag{20}$$

The dissociation of DT is neglected, the atomic and ionic partition functions $Q_{0,1}$, are taken as unity, T_{eV} is the temperature in electron-volts, and the ionization potential is E_I = 13.6 eV.

III. RESULTS

The conditions where DT fusions might be generated in the course of a compressional heating driven by the liquid forces transferred to a collapsing gas-filled cavity are explored at two levels using the simplified model described in Sec. II. At the parametric level, the "disequilibrium" parameter f_{eq} along with and initial equilibrium bubble radius, R_o^{EQ}, are specified to determine an initial normalized radius, $x_o = R_o/R_o^{EQ}$, with which to begin the time-dependent calculation of R(t) and the fusion-related integral and peak parameters. At the second level, the Rayleigh-Plesset equation, Eqn. (9), is solved for an initially equilibrium bubble with a radius R_o^{EQ} chosen to assure that the natural resonance

frequency, $\omega_r = \sqrt{(P_h / \rho_\ell)} / R_o^{EQ}$, matches that of the drive frequency, $2 \pi f$, where $P_a(t) = P_A \sin (2 \pi f t)$. A second, aharmonic/resonant drive scenario was also investigated, wherein $P_a(t)$ is applied only during a given bubble collapse at a value that is double the value used to drive a previous collapse. For either of these harmonic- or aharmonic/resonant-driven simulations, the value of f_{eq} prior to each collapse is recorded and correlated with the fusion performance [*e.g.*, x_{min}, $T_{keV}(x_{min})$, $<n\tau\ T_{keV}>$, and YLD]. For all computations a van der Waals equation of state is used, and the correction for (accumulated) radiation losses embodied in Eqns. (16)-(20) is imposed. The fixed parameters listed in Table I are used, which generally reflects the properties of water at T_o = 300 K.

A. Correlation Based on Specification of Disequilibrium Parameter, f_{eq}

Figure 1 gives a schematic representation of the case wherein an equilibrium ($x = 1$, $f_{eq} = 1$) bubble is brought by some unspecified route to a state of disequilibrium ($f_{eq} < 1$), the resulting three-dimensional "sling shot" is released, and the ensuing compression (and rebound) is numerically followed in time. The unspecified (unmodeled) equilibrium $\rightarrow$ disequilibrium trajectory, $x = 1 \rightarrow x_o$ is assumed to occur slowly (relative to the time scale of the ensuing collapse) and isothermally; the initial conditions used for the modeling of the bubble collapse in terms of the equilibrium ($x = 1$, $f_{eq} = 1$) state are as follows:

$$P_{go} = f_{eq}\ P_{go}^{EQ}\ ;$$

$$R_o = R_o^{EQ} / f_{eq}^{1/3}\ ; \tag{21}$$

$$T_o = T_o^{EQ}\ .$$

The state conditions upon peak (adiabatic) compression are approximately given by

$$P_g = P_{go}^{EQ} / f_{eq}^{\,1/(\gamma\ -1)}\ ;$$

$$R = r_o^{EQ}\ \ f_{eq}^{(2-\gamma)/3/(\gamma-1)}\ , \tag{22}$$

$$T = T_o^{EQ} / f_{eq}\ .$$

The product of peak pressure, $\sim nT_{keV}$, and the collapse time, τ^*, given by Eqn. (7) scales as follows:

$$\frac{n\tau^* T}{(n\tau T)_o} = \frac{1}{f_{eq}^{(2+\gamma)/3(\gamma-1)}}\ , \tag{23}$$

where

$$(n\tau^* T)_o = \frac{N_A\ k_B}{R_G}\ (\omega_r \tau^*)\ \sqrt{P_h\ \rho_l}\ , \tag{24}$$

and from Eqn. (7), $\omega_r \tau^*$ is near unity. These relationships are based solely on equilibrium conditions and are given only as an indication of key scaling dependencies in the search for means to maximize T and $<n \tau T_{keV}>$.

All computations that varies f_{eq} parametrically correspond to an equilibrium bubble of radius $R_o^{EQ} = 100$ μm, with the isothermal excursion to the initial radius R_o where actual modeling of the bubble collapse begins, being given by

$$x_o = \left[\frac{1/f_{eq} + v_H^*}{1 + v_H^*} \right]^{1/3} . \qquad (25)$$

In this expression, $x_o = R_o/R_o^{EQ}$, $v_H^* = \rho_o v_H$, and $\rho_o = (P_h + P_{\sigma o} - P_{vo})/(R_G T_o)$ is the (DT) gas density in the equilibrium (x = 1) bubble; for all cases, the Table-I parameters are used, along with $P_h = 1 \times 10^5$ Pa and $P_{\sigma o} = 2\sigma/R_o^{EQ}$.

The parametric dependencies of $x_{min}/x_o = R_{min}/R_o$, $<n\tau T>/10^{20}$, YLD/10^6, and $T(x_{min})$ on f_{eq} are shown on Fig. 2. The sample normalized-radius trajectory (during compression) used in the Fig.-1 illustration corresponds to $f_{eq} = 0.01$. Shown also is the f_{eq} dependence of $x_{min} = R_{min}/R_o^{EQ}$. The peak temperatures reported correspond to an adiabatic heating along an adiabat that starts with a disequilibrium bubble at $T_o = 300$ K, under the assumption that the equilibrium → disequilibrium trajectory was achieved slowly and isothermally; the $T \sim 1/f_{eq}$ dependence suggested by Eqn. (22) is indicated. Shown also on Fig. 2 are temperatures for the case where the expansion part of the trajectory was also adiabatic; that is, the expansion from x = 1 to $x = x_o$ was accompanied by a cooling prior to the subsequent bubble collapse and adiabatic compressional heating. [*e.g.*, neglecting the van der Waals correction, which is small in this region, $T_o = T_o^{eq}/(x_o^{3(\gamma-1)})$]. The $<n\tau T>$ and YLD values reported on Fig. 2, however, correspond to the more optimistic isothermal equilibrium → disequilibrium trajectory. For this case, measurable quantities of neutrons from a single bubble collapse would require that bubble to be "set up" with $f_{eq} < 10^{-4}$. Considerable lower values of f_{eq} would be required if the assumed expansion from the equilibrium to the disequilibrium state is adiabatic, as will be seen from the following evaluations of the Rayleigh-Plesset equation to describe an initially equilibrium bubble trajectory to disequilibrium and subsequent collapse under a range of externally driving pressures.

B. Correlations for Driven Equilibrium Bubbles

1. Harmonic Drive [$P_a = P_A \sin(2\pi f t)$]

The radius trajectory of an (initially) equilibrium bubble subjected to $P_A = 5 \times 10^5$ Pa pressure oscillations at an f = 10-kHz frequency is shown on Fig. 3. For this case, the (initially) resonant bubble has a radius $R_o^{EQ} = 292$ μm when $P_h = 1 \times 10^5$ Pa. Comparing $x = R/R_o^{EQ}$ to the driver pressure, also given as $1 + P_a(t)/P_h$ on Fig. 3, indicates an initially harmonic, but highly non-linear, response that is followed by the bubble trajectory settling

onto a moderately rhythmic forth subharmonic. Fairly deep compressions (limited by the van der Waals equation of state) from $f_{eq} \sim 0.5\text{-}1.0\times10^{-4}$ disequilibria are predicted for these sinusoidally driven bubbles. The correlation of x_{min}, $T(x_{min})$ and $<n\tau T>$ with the computed f_{eq} values taken from the Fig.-3 trajectories just prior to a given collapse is shown on Fig. 4. The relatively low (peak) temperatures for even low values of f_{eq} result from the adiabatic cooling computed during the expansion part of the trajectory, as well as the cumulative effects of radiation cooling for this constant-amplitude sinusoidal drive. The impact of elimination of radiative losses is also shown on Fig. 4; the accumulated radiation losses impact primarily those deep compressions that occur later in the chain of compressions depicted on Fig. 3. As for the cases where the bubble is forced to begin to collapse from a specified f_{eq} value (Sec. III.A.), the van der Waals equation of state limits the maximum compressions permitted. The neutron yield, YLD, for all compressions registered on Fig. 3 are below the minimum scale used on Fig. 4 for this $P_A = 5\times10^5$-Pa harmonic-drive case; a means must be found to pump more energy into the collapsing bubble while forcing it to higher levels of disequilibrium prior to collapse.

2. Aharmonic/Resonant Driver

Just as more energy and greater excursions can be transferred to a ball tethered to a paddle by an elastic band through timely swats, so can tailoring of the impulse to the anharmonic trajectory of the bubble radius increase the response and performance. Figure 5 gives the time dependence of the normalized bubble radius and drive pressure for the case reported in Sec III.B.2., but with pressure being applied only once the bubble collapse commences. Furthermore, this aharmonic application of pressure is doubled in intensity for each subsequent collapse, with P_a starting at 1×10^5 Pa. The values of x_{min}, $T(x_{min})$, $<n\tau T>$ and YLD for each bubble collapse registered on Fig. 5 is shown on Fig. 6 as a function of the respective value of f_{eq} just prior to collapse. The impact of (cumulative) radiation loss is not as great as that reported of the harmonic drive because of the ratcheting of the applied pressure in the aharmonic/resonant case. The neutron yields, however, remain low unless $f_{eq} < 10^{-6}$ primarily because of the low (peak) temperatures related to the adiabatic cooling during each expansion to the disequilibrium state that proceeds a give bubble collapse. Generally, the assumption of fully adiabatic expansion (and cooling) leads to unrealistically low temperatures prior to collapse and requires an improved model.[24]

IV. SUMMARY

The collapse of a gas-filled bubble in disequilibrium can occur with a significant focusing of energy onto the entrapped gas in the form of pressure-volume work and/or acoustical shocks. The suggestion that extreme conditions necessary for nuclear fusion may be possible[1,7,11] been examined parametrically in terms of the ratio f_{eq} of initial bubble pressure relative to that required for equilibrium. The disequilibrium bubble is viewed as a three- dimensional "sling shot" loaded to an extent allowed by the maximum level of disequilibrium that can stably be achieved. Values of this disequilibrium ratio in the range $f_{eq} = 10^{-5} - 10^{-6}$ are predicted by an idealized bubble-dynamics model as necessary to achieve conditions where nuclear fusion of deuterium-tritium might be observed. Harmonic and aharmonic pressurizations/decompressions have been examined as means to achieve the required levels of disequilibrium, with the latter drive scenario offering a possible means to achieve f_{eq} values and peak temperatures where measurable quantities of fusion

might occur. While the simplified "adiabatic" compressional model uses a hard-sphere equation of state and allows for Bremsstrahlung losses, any number of the phenomena listed in Sec. II. and not included in this analysis could impact these predictions in a generally negative way. The creation of multiple and interacting gas-phase shock waves and mechanisms that allow isothermal expansions to the disequilibrium state could enhance the predictions of relatively low fusion yields, however; an improved understanding of the potentially positive impact (from the view point of heating, density amplification, and increased fusion yield) of multiple interacting shocks is suggested as a course for future work, as well as the incorporation of gradient-driven transport, gas/plasma-wall interactions, and an improved radiation model.

REFERENCES

1. L. A. Crum, "Sonoluminescence," Physics Today, p. 22, (September 1994).

2. L. A. Crum and R. A. Roy, "Sonoluminescence," Science, **266**, 233 (1994).

3. Sonochemistry Special Issue, Ultrasonics, **30**(3) (1992).

4. T. J. Mason and J. P. Lorimer, Sonochemistry: Theory, Applications and Uses of Ultrasound in Chemistry, Ellis Horwood Limited, Chichester UK (1984).

5. K. S. Suslick, "The Chemical Effects of Ultrasound," Scientific American, p. 80 (February 1989).

6. M. A. Margulis, "Fundamental Aspects of Sonochemistry," Ultrasonics, **30**(3), 4 (1992).

7. M. A. Margulis, "Modern Views on the Nature of Acousto-chemical Reactions," Russ. J. Phys. Chem. **50**, 1 (January 1976) [translated from Zhurnal Fisicheskoi Khimii, **50**, 1-18 (1976)].

8. A. Waltson and G. T. Reynolds, "Sonoluminescence," Adv. in Physics, **33**(6), 595 (1984).

9. Acoustic Cavitation Series (6 parts), Ultrasonics, **22**(1), 25; **22**(2),67; **22**(3), 115; **22**(4), 145; **22**(5), 215; **22**(6), 261 (1984).

10. K. S. Suslick, **Ultrasound: Its Chemical, Physical, and Biological Effects**, VCH Publishers, Weinheim, Germany (1988).

11. B.P. Barber, C. C. Wu, R. Loefstedt, P. H. Roberts, and S. J. Putterman, "Sensitivity of Sonoluminescence to Experimental Parameters," Phys. Rev. Lett., **72**(9), 1380 (1994).

12. H. G. Flynn, "Cavitation Dynamics. I. A Mathematical Formulation," J. Acoust. Soc. Am., **57**(6) (1975).

13. T. J. Leighton, **The Acoustic Bubble**, Academic Press Limited, London (1994).

14. H. P. Greenspan and A. Nadim, "On Sonoluminescence of an Oscillating Gas Bubble," Phys. Fluids, **A5**(4), 1065 (1993).

15. C. C. Wu and P. H. Roberts, "Shock-Wave Propagation in a Sonoluminescing Gas Bubble," Phys. Rev. Lett., **70**(22), 3424 (1993).

16. C. C. Wu and P. H. Roberts, "A Model of Sonoluminescence," Proc. Roy. Soc., London, **445**, 323 (1994).

17. L. Frommhold and A. A. Atchley, "Is Sonoluminescence due to Collision-Induced Emission?," Phys. Rev. Lett., **73**(21), 2883 (1994).

18. M. Krech, **The Casimir Effect in Critical Systems**, World Scientific Publishers, Singapore, (1994).

19. J. Schwinger, "Casimir Light: The Source," Proc Natl. Acad. Sci., **90**, 2105 (1993).

20. Lord Rayleigh, "On the Pressure Development in a Liquid During the Collapse for Spherical Cavity," Phil. Mag., **34**(6), 94 (1917).

21. Ya. B. Zel'dovich and Yu. P. Raizer, **Physics of Shock Waves and High-Temperature Hydrodynamic Phenomena**, Academic Press, N.Y. (1966).

22. M. I. Boulos, P. Fauchais, and E. Pfender, **Thermal Plasmas: Fundamentals and Applications**, Plenum Press, N.Y, (1994).

23. R. A. Krakowski, "Dynamics of a Cavity Under Acoustic Loadings: A Parametric Study," Los Alamos National Laboratory document LA-UR-94-3804, (November 9, 1994).

24. T.V. Prevenslik, "Sonoluminescence Induced Deuterium Fusion," Trans. Fus. Technol., **26**(12), 530 (1994).

NOMENCLATURE

$c(m/2)$	sound speed in gas
$c_{p,v}(J/kg/K)$	gas heat capacities at constant pressure,volume
$C_{BR}(W\ m^3/keV^{1/2})$	Bremsstrahlung radiation coefficient, 4.8×10^{-37}
$E_I(eV)$	(hydrogen) ionization potential
$e(J/eV)$	electronic charge
$f(Hz)$	driver frequency
f_{eq}	disequilibrium parameter, P_{go}/P_{go}^{EQ}
f_{ion}	(Saha) ionization fraction, Eqn. (18)
f_{VDW}	van der Waals correction, Eqn. (15)
$g(z)$	pressure-volume work function, Eqn. (6)
$h(Js)$	Planck's constant, 6.6252×10^{-34}
I	radiation integral, Eqn. (15)
K	Saha function, Eqn. (19)
$k_B(eV/K)$	8.617×10^{-5}
$KE(J)$	kinetic energy
$\dot{M}(kg/s)$	mass flow of liquid towards collapsing bubble
$m_e(kg)$	electron rest mass, 9.1083×10^{-31}
N	number of a series of sequential bubble compressions
$N_A(entities/mole)$	Avagadro's number, 6.0249×10^{24}
$n(1/m^3)$	gas particle density, $\rho_g N_A$
$<n\tau T>(s\ keV/m^3>$	time-averaged gas pressure during a given bubble collapse
$P_a(Pa)$	acoustic (time-varying) pressure exerted on cavity
$P_A(Pa)$	amplitude of acoustic (time-varying) pressure exerted on cavity
$P_{g,go}(Pa)$	gas (non-condensible) pressure in cavity
P_g^{EQ} (Pa)	gas (non-condensible) pressure in cavity for equilibrium bubble
$P_h(Pa)$	hydrostatic (constant background) pressure exerted on cavity
$P_{v,vo}(Pa)$	vapor pressure (of liquid) in cavity
P_σ (Pa)	effective surface-tension pressure, $2\ \sigma/R$
$PE(J)$	potential energy
$p_{RAD}(W/m^3)$	(Bremsstrahlung) radiation power density
$Q_{0,1}$	partition function for atom,ion
$R(m)$	bubble/cavity radius
$R_G(J/kg/K)$	gas constant, 8,317.
$r(m)$	radial coordinate into liquid
$R_o(m)$	initial bubble/cavity radius
R_o^{EQ} (m)	initial cavity radius for equilibrium bubble
$S(J/K)$	enthalpy
$t(s)$	time
$T(K)$	temperature of gas
$T_o(K)$	reference (initial) temperature of gas
$T_{crit}(K)$	thermodynamic critical temperature of water
$T_{eV}(eV)$	gas/plasma temperature in electronvolts

T_{keV}(keV)	gas/plasma temperature in kiloelectronvolts
$V_o(m^3)$	initial volume of bubble, $(4/3)\pi R_o^3$
$v(m^3/kmole)$	gas molecular (atomic) volume, 1/r
v_H	$(m^3/kmole)$ molecular (atomic) volume
v_H^*	normalized molecular (atomic) volume, $v_H \rho_{go}$
VDW	van der Waals correction, Eqn. (14)
$w(J/m^3)$	gas/plasma-phase energy density
x	radius compression ratio, R/R_o^{EQ}
x_o	normalized disequilibrium radius, R_o/R_o^{EQ}
YLD	number of (DT) fusions per bubble collapse
Z	atomic number of ionized gas
z	volumetric compression ratio, $(R_o/R)^3$
z_{max}	maximum compression (dR/dt = 0)
ΔH(J/mole)	heat of vaporization
η(kg/m/s)	liquid viscosity
γ	gas heat-capacity ratio
$\Gamma(y)$	Gamma function
σ(N/m)	surface tension of liquid
$<\sigma v>(m^3/s)$	(DT) fusion reactivity
ω(rad/s)	driver frequency, $2\pi f$
ω_r(rad/s)	bubble resonance frequency, $\sqrt{(P_h/\rho_\ell)}/R_o$
$\rho_\ell(kg/m^3)$	liquid density
$\rho_g(kmole/m^3)$	gas density
τ(s)	bubble natural response time, or nominal inertial confinement time (as in $<n\tau T>$)
τ^*(s)	collapse time of a pressureless cavity

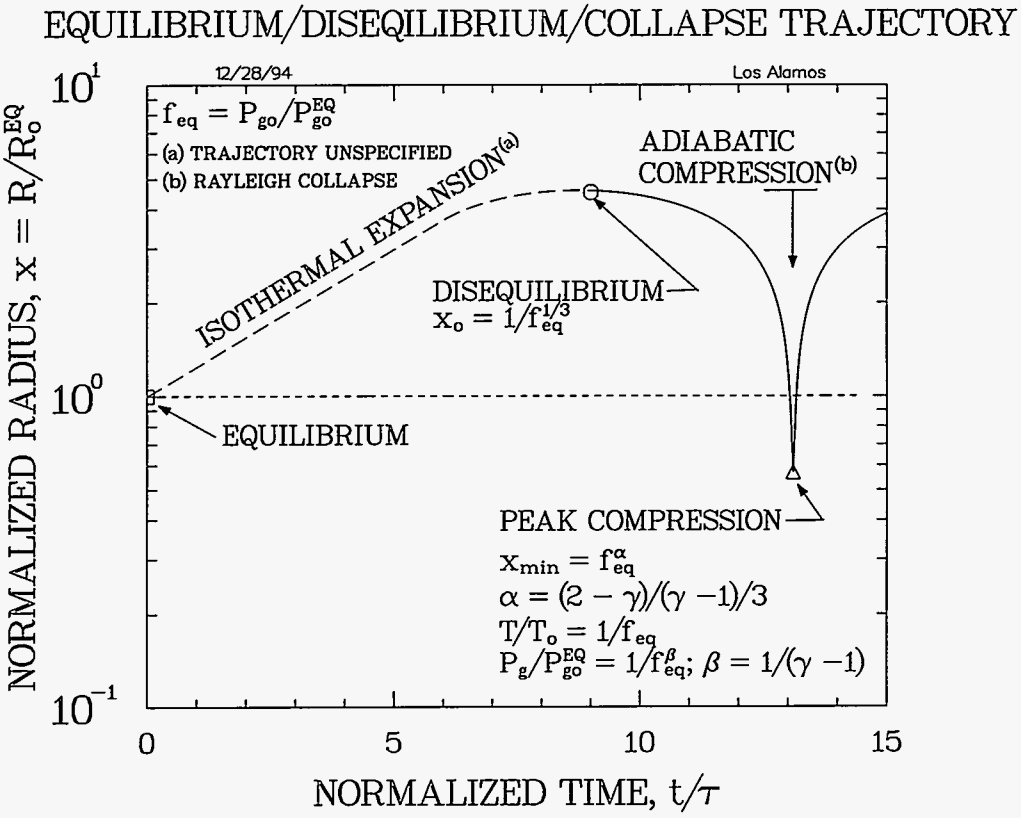

Figure 1. Schematic diagram of bubble radius trajectory illustrating approach to $f_{eq} < 1$ disequilibrium from f_{eq}, x = 1 equilibrium state, followed by collapse to x_{min}.

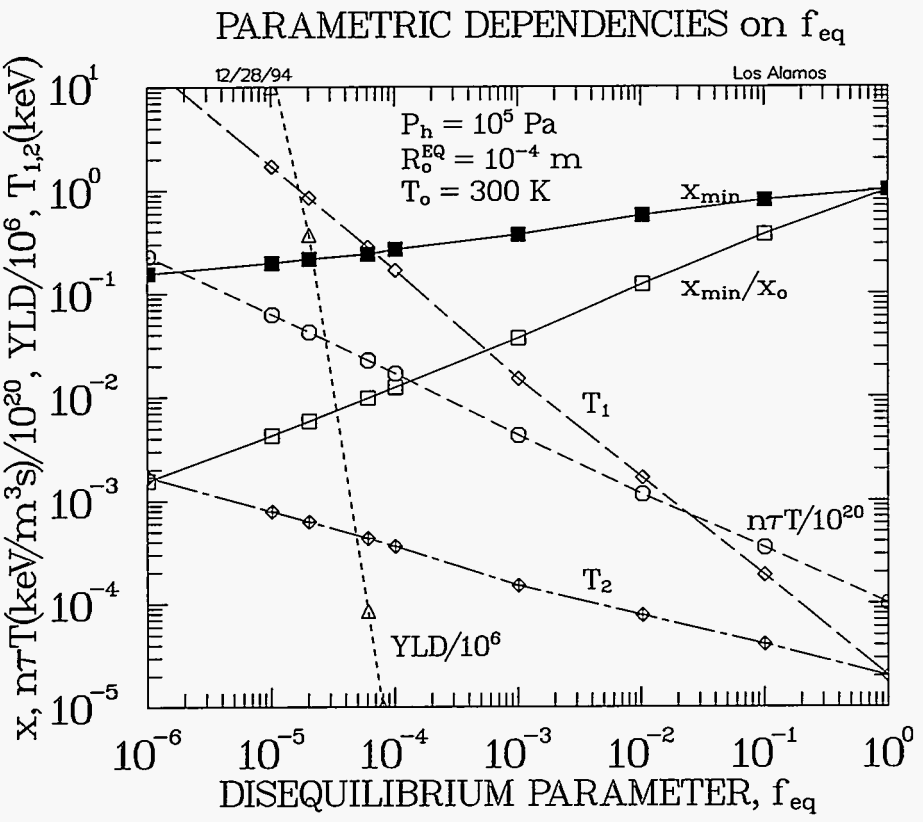

Figure 2. Parametric dependence of integral and peak-compression parameters on disequilibrium parameter, $f_{eq} = P_{go}/P_{go}^{EQ}$.

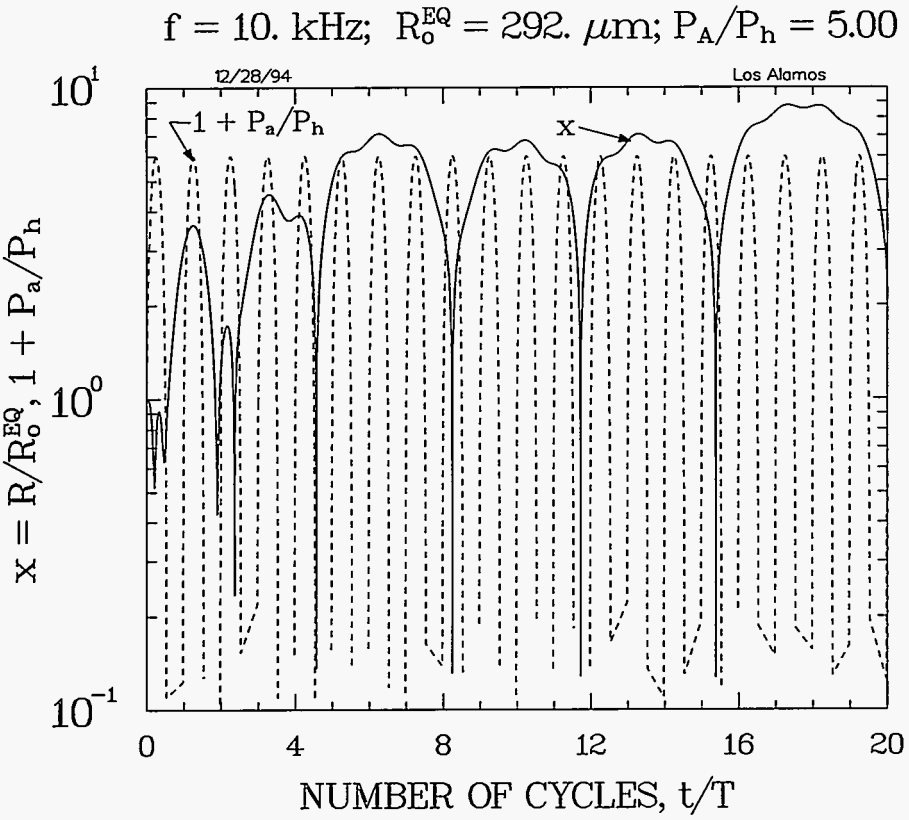

Figure 3. Response of normalized bubble radius to f = 10 kHz, $P_A = 5\times10^5$ Pa sinusoidal pressure oscillations starting with a resonant ($\omega_r = 2\pi f$), equilibrium ($x, f_{eq} = 1$) bubble.

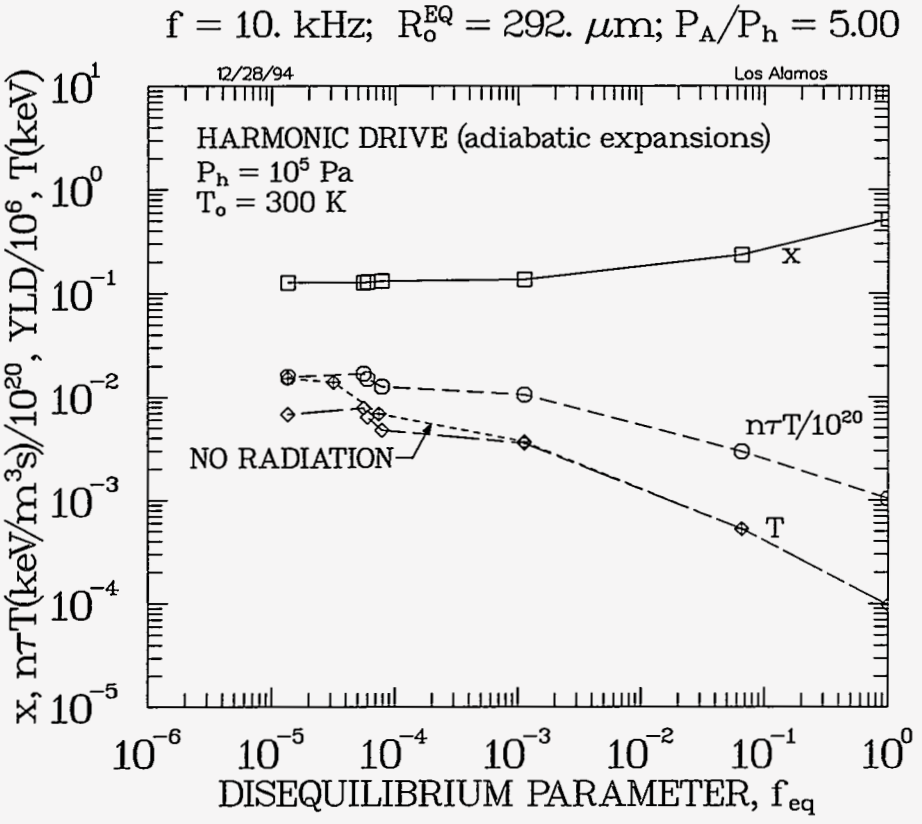

Figure 4. Dependence of integral and peak-compression parameters for the harmonically driven bubble compressions given on Fig. 3.

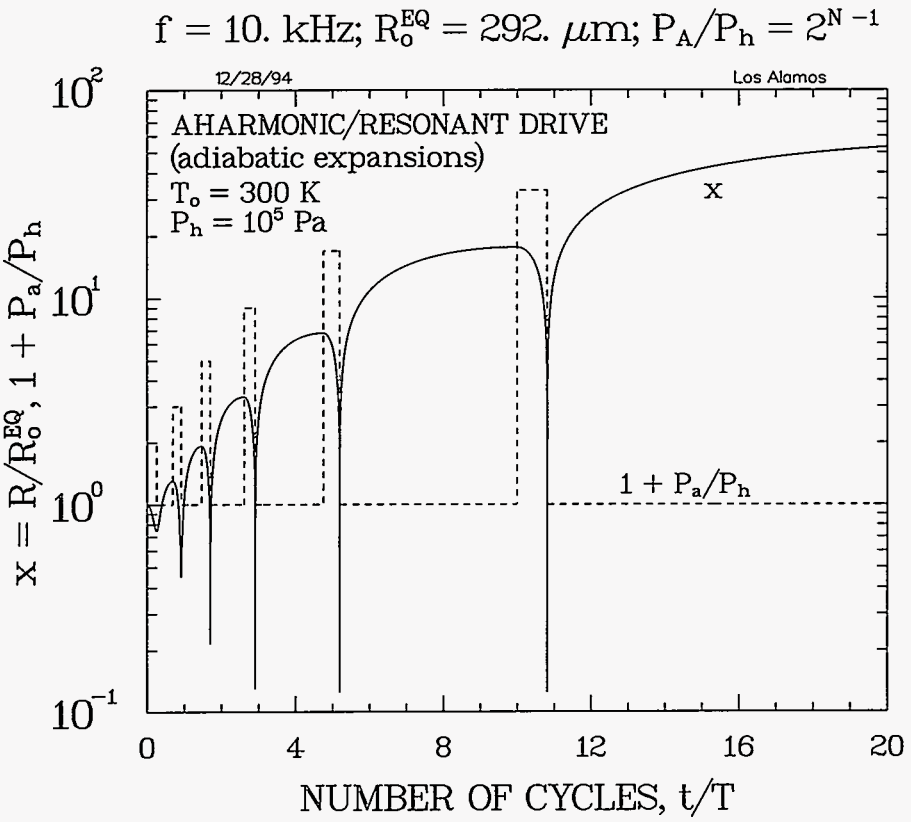

Figure 5. Response of normalized bubble radius to progressively doubled pressure pulses for conditions that are otherwise identical to those used for the harmonically driven case given on Fig. 3.

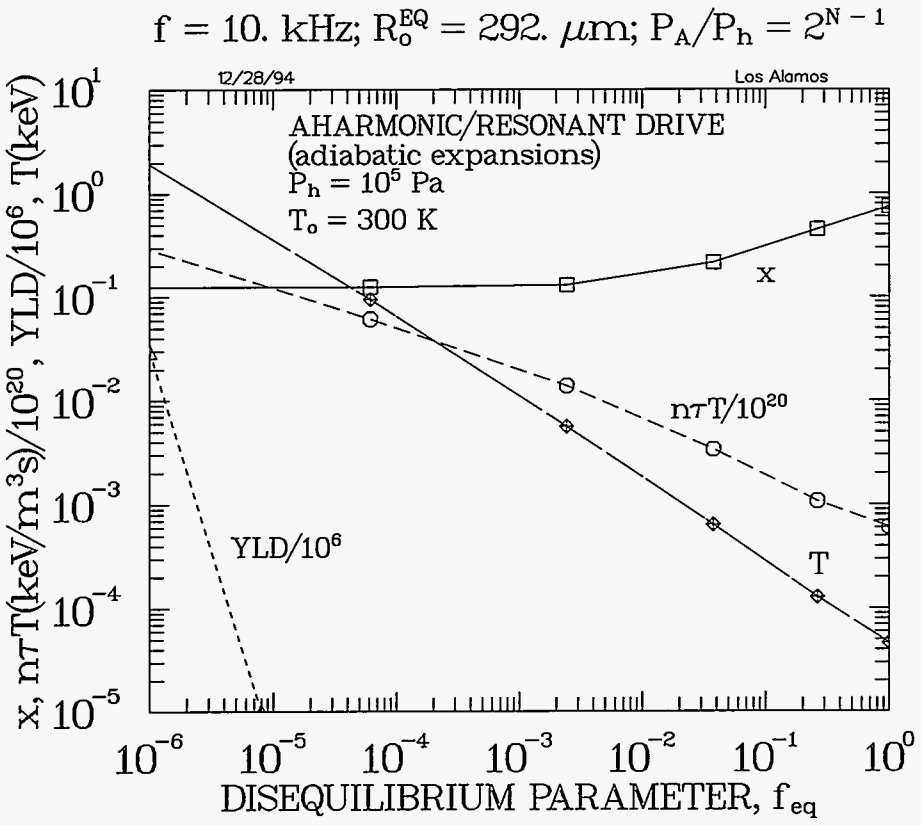

Figure 6. Dependence of integral and peak-compression parameters for the aharmonic/resonant drive given on Fig. 5.

Table I Input Parameters

Liquid density, ρ_ℓ(kg/m^3)	988.
Background hydrostatic pressure, P_h(Pa)	1.00×10^5
Vapor pressure at T_o = 300 K, P_{vo}(Pa)	4.21×10^3
DT molecular volume, v_H(m^3/kmole)	0.05
Heat-capacity ratio, γ	1.67
Surface tension, σ (Nm)	0.0729
Fluid viscosity, η (kg/m s)	0.00
Reference temperature, T_o(K)	300.
Critical temperature, T_{crit}(K)	647.
Ionization potential, E_I(ev)	13.6
Atomic number of ionized gas, Z	1.0
Partition functions for neutral, ionic species, $Q_{0,1}$	1.0,1.0